AIAA 80-1784R

# Space Telescope Pointing Control System

H. Dougherty*
*Lockheed Missiles & Space Company, Inc., Sunnyvale, Calif.*
K. Tompetrini† and J. Levinthal‡
*Bendix Guidance Systems Division, Teterboro, N.J.*
and
G. Nurre§
*NASA Marshall Space Flight Center, Huntsville, Ala.*

**The Space Telescope is a free-flying spacecraft designed for space shuttle launch. The Space Telescope's pointing control system slews the optical axis from one target star region of the celestial sphere to the next, and maintains precision pointing for the target star for up to 24 hours. The spacecraft digital computer processes the precision attitude and rate sensor data to generate torque commands for the reaction wheels. The pointing control system has four major elements: the command generator, the control system, the attitude reference processing, and momentum management. The emphasis is on relating design requirements to the hardware and software implementation.**

## Introduction

THE Space Telescope, shown in Fig. 1, has a 2.4-m telescope designed to allow scientists to observe the universe with a clarity and to distances never before achieved. The Space Telescope observatory performance objectives require stabilizing the telescope to allow near-diffraction limited images to be obtained, to maintain the pointing stability for 10 h of observation, which may require 24 h of actual time, and to allow precision tracking of solar objects.[1,2]

The Space Telescope pointing control system is designed to meet the fine pointing performance of 0.007 arc-sec stability, maneuver the telescope 90 deg in 18 min, or less, and provide the capability for deployment from, and retrieval by, the space shuttle. The pointing control system objectives are met using fine guidance sensors for attitude information to achieve fine pointing, rate gyro assemblies for rate and short-term attitude information, reaction wheel assemblies sized to provide both the torque required for maneuvering and the precision control torques during fine pointing, and magnetometers and magnetic torquers for momentum management. A digital computer is used to calculate the control law, attitude reference, momentum management law, and command generator. The command generator shapes the acceleration and incremental angle commands to the control system to limit structural mode excitation. Attitude information also can be provided by the fixed head star trackers and sun sensors. In case of failures of certain elements of the primary control system, a backup gyro package and backup control system with its associated electronics are provided.

The pointing control system provides the capability for autonomous maneuvering, acquisition, and fine pointing based on time-tagged stored program commands, as well as the ability for real-time interactive commands from the Space Telescope Operations Control Center. All commands requiring motion of the vehicle and/or fine guidance sensor guide stars are processed through the command generator to ensure adequate smoothing of the motions, ensuring that the interferometers remain locked and fine pointing requirements are met.

## Overview

The pointing control system operational modes derive from a consideration of the mission. The initial Space Telescope mission contains the following five scientific instruments: the wide-field planetary camera, the faint object camera, the faint object spectrograph, the high-resolution spectrograph, and the high-speed photometer. In addition, since there are three fine guidance sensors, the fine guidance sensor not being used for pointing control system control can be used for astrometry, i.e., the precise measurement of the relative positions of stars. The astrometry accuracy is anticipated to be an order of magnitude improvement over ground-based measurements. The Space Telescope is deployed from the shuttle orbiter in a nominal 500-km, 28.5-deg inclination orbit. The tipoff rates imparted to the Space Telescope by the release from the orbiter are less than 0.1 deg/s for each axis. The four reaction wheels damp this rate, and the Space Telescope captures the sun via the sun sensors. Because of power considerations, the sun orientation will be maintained in the $-V_1$ axis direction. The Space Telescope Operations Control Center communicates to the Space Telescope via the synchronous altitude tracking and data relay satellite system and determines more precise Space Telescope attitude using the fixed head star trackers.

Additionally, the Space Telescope Operations Control Center calibrates the gyro bias and scale factor and the gyro input axis to fixed head star tracker line of sight. The rate gyros are located with the fixed head star tracker on a platform on the optical telescope assembly. Once these calibrations are completed, the (fine guidance sensor)-to-(rate gyro/fixed head star tracker) calibrations are performed. Upon completion of calibrations, the pointing control system is ready to maneuver star-to-star and perform star observations, planet tracking, or serpentine scan patterns, as required, to obtain scientific data.

The pointing control system design is driven by the following considerations.

1) *Structural modes:* The solar array and optical telescope assembly modes have large modal coefficients. For example, the value of the solar array inertia about the Space Telescope center of mass is almost one-half that of the Space Telescope

Presented as Paper 80-1784 at the AIAA Guidance and Control Conference, Danvers, Mass., Aug. 11-13, 1980; submitted Jan. 21, 1981; revision received Feb. 2, 1982. 

*Manager, Pointing Control Subsystem, Space System Division. Member AIAA.
†Pointing Control System Engineering Manager. Member AIAA.
‡Manager, Systems Engineering.
§Branch Chief, Pointing Control System, System Dynamics Laboratory.

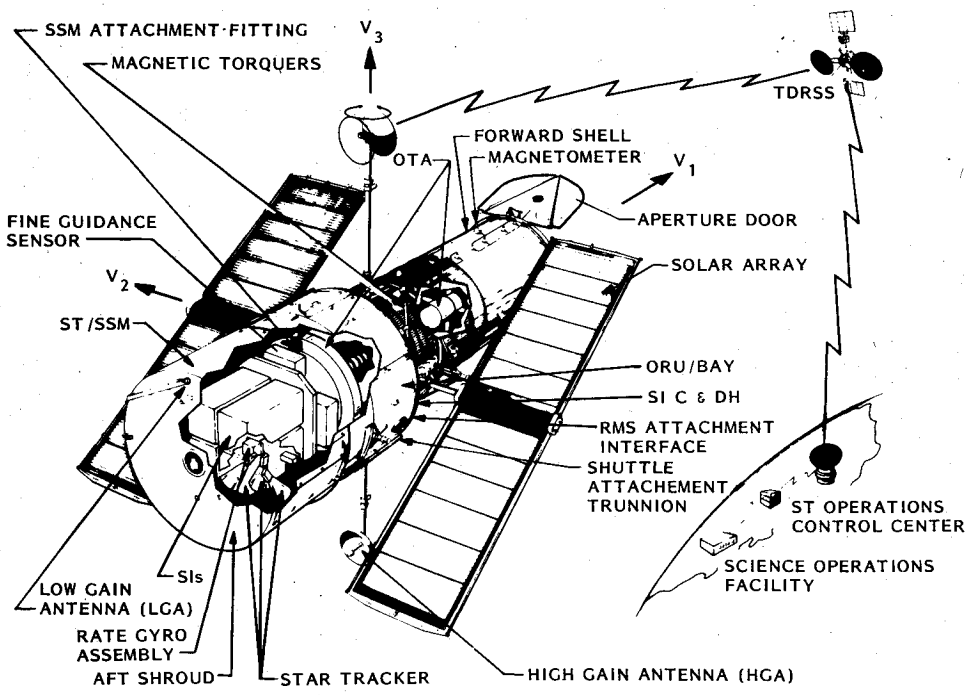


**Fig. 1 The Space Telescope system.**

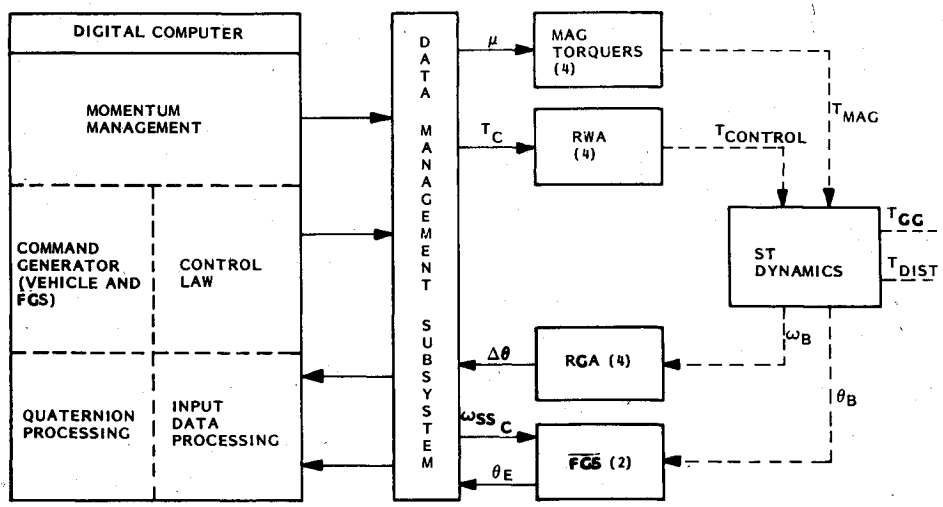


**Fig. 2 Primary control system.**

centerbody, which comprises the support systems module and optical telescope assembly. The control system sample rate and compensation are chosen to stabilize the modes. The command generator shapes maneuvers to limit structural excitations during maneuvers.

2) *Dynamic control range:* The orbiter tipoff rates are 0.1 deg/s or less. The fine pointing performance is on the order of 0.007 arc-sec. These values require a large dynamic range in the rate gyros and reaction wheels to ensure transition from large rate capture capability to fine pointing.

3) *Limited fine guidance sensor fine pointing range:* The fine guidance sensor uses an interferometer as part of the precision sensor.[3] The interferometer has a useful range of approximately $\pm 0.02$ arc-sec, which requires that the control system errors and Space Telescope torque disturbances be limited to ensure that the pointing control system does not cause disturbances that exceed the interferometer range.

4) *Redundancy:* Orbiter capture with up to two pointing control system failures, e.g., gyros, reaction wheels. Additionally, the Space Telescope autonomously "safes" the vehicle if there is a threat to the operation and subsequent orbiter capture. This leads to the need for software backup modes as well as hardware modes. The pointing control system uses the same functional form for the software control modes, modifying the control system parameters as required for the specific operational mode.

The primary mission operation, i.e., fine pointing, is performed using the primary pointing control system mode consisting of the fine guidance sensors, rate gyros, and reaction wheels. The backup software modes use the rate gryos and reaction wheels.

## Primary Mode

The major elements of the primary pointing control system mode are shown in Fig. 2. The control system is based on the low-cost design configuration.[4] The sensors used are the rate gyro assembly and the fine guidance sensors. The rate gyro assemblies comprise six rate integrating gyros configured in quantized pulse width modulated rebalance loops and contained in three sensor units consisting of two gyro channels each. A two-channel unit comprises a rate sensor unit and an electronics unit. The gyro has a dual rate range. The high rate scale range is 0.5 deg/s with a pulse weight of 0.015 arc-sec, and the low rate scale is 20 arc-sec/s with a 0.00025 arc-sec pulse weight.

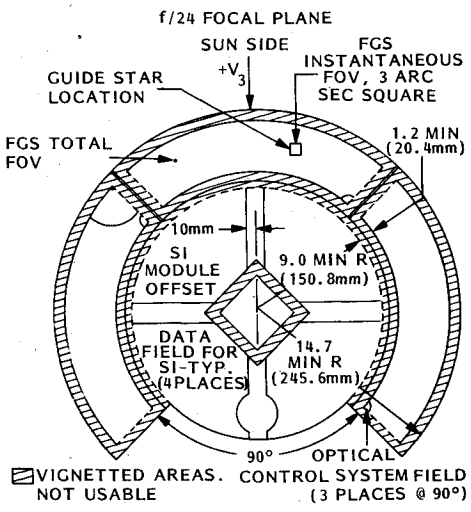


**Fig. 3 Optical telescope assembly focal plane.**

There are three fine guidance sensors, two of which are used by the pointing control system for attitude update purposes when pointing or performing low rate scans. The fine guidance sensors share the optical telescope assembly field of view with the scientific instruments shown in Fig. 3. The scientific instruments' fields of view occupy the inner 9 arc-min of the focal surface. Each fine guidance sensor has a total field of view of about 60 arc-min$^2$. The four photomultiplier tubes are used for both acquisition and fine pointing. In fine pointing mode, the photomultiplier tubes are used in an interferometric mode. Because of the limited dynamic range (approximately $\pm 0.02$ arc-sec) of the interferometer, the fine guidance sensor uses the sum output of the photomultiplier tubes to achieve fine guidance system acquisition after the pointing control system slews the line of sight of the Space Telescope from one target star to the next. The fine guidance sensor contains star selectors, which are effectively rate control systems containing rotating prisms, to allow the 3 arc-sec$^2$ instantaneous field of view of the photomultiplier tubes to be maneuvered over the total 60 arc-min$^2$ field of view of the fine guidance sensor.

Four reaction wheel assemblies generate control torques. The input axes of the rate gyros and torque-producing axes of the reaction wheels are skewed relative to the Space Telescope line of sight coordinates to provide system redundancy. Thus, the pointing control system loop can operate using only three gyro channels and three reaction wheels. The reaction wheel has a 0.8 N-m torque capability, 3000 rpm maximum speed, and 0.84 kg-m$^2$ rotor inertia.

The pointing control system contains three fixed head star trackers and sun sensors. The fixed head star trackers have $8 \times 8$ deg$^2$ fields of view and sensitivity down to 5.7 magnitude stars.

The two magnetometers are three-axis, flight-proven units. The four magnetic torquer bars are each 2.1 m long and produce approximately 0.3 N-m of torque.

The computer has six 8K 24-bit words, plated wire memories, three central processing units, and three input/output channels. The data management subsystem contains a data management unit, which has special data interfaces for the rate gyros and fixed head star trackers, and digital interface units. The digital interface units can send and receive 16-bit serial digital words. They interface with all data except that of the rate gyros and fixed head star trackers data output.

The attitude reference processing interfaces with the fine guidance sensor and fixed head star tracker data to generate attitude update commands to the control system. The Space Telescope Operations Control Center determines the desired locations of the stars in the field of view of the fine guidance sensor and fixed head star tracker in the coordinate axes suitable to their sensor geometry. For example, desired star locations in the fixed head star tracker would be given in the vertical and horizontal coordinates of the tracker. The attitude reference processing determines the error between the desired and actual star locations and calculates the attitude correction in vehicle coordinates. Depending on the magnitude of the correction, it is either slowly "leaked" into the control system, e.g., via an exponential function, or, if the error is large, the command generator performs a maneuver to remove the error. The leak-in time constants and maneuver time are selected to both limit structure mode excitation and prevent control system saturation.

The command generator shapes the vehicle jerk (derivative of acceleration) using the equivalent of a "$1-\cos$"-shaped jerk pulse. This generator is used for all maneuvers, e.g., star-to-star maneuvers, solar object tracking, and serpentine scanning. The lower bound on solar array frequency is approximately 0.05 Hz; hence, the jerk pulse width is normally 1 min. The command generation sends acceleration feed forward and incremental angle commands to the vehicle control system and rate commands to the fine guidance sensor star selectors, if required as, for example, during solar object tracking.

The input to the control system shown in Fig. 4 is the command generator acceleration and incremental position commands, rate gyro assembly "incremental" angles per 25 ms and the fine guidance sensor angle output for attitude. The rate gyro assembly data can be used for both rate and short-term attitude. The control system uses position, rate, and integral compensation. A digital filter is used in the rate path to suppress Space Telescope structural modes. The optical telescope assembly modal parameter values are large and require suppression to maintain adequate stability margins. An estimate of external torque is used to eliminate the cross-coupling between axes, effectively decoupling $V_1$, $V_2$, and $V_3$ control torques. The acceleration command effectively goes directly to the reaction wheel torquers and puts an instantaneous torque on the vehicle. The reaction wheel torque response is governed only by the feed forward path, which has a bandwidth of approximately 80 Hz. Therefore the vehicle follows the shaped acceleration commands. The feedback provides an error correction path to account for variances in parameters such as the vehicle inertia estimate and the reaction wheel feed forward gain. A closed loop on the reaction wheel provides compensation to overcome the bearing drag torque and has a bandwidth of approximately 0.1 rad/s.

The control loop is a high gain system and can be torque-saturated for unsmoothed external torques, attitude updates, or movement of fine guidance sensor star selectors. For example, in fine pointing, the attitude gain is about 3.5 N-m/arc-sec, resulting in loop saturation at about 0.5 arc-sec for the four-reaction wheel case and 0.2 arc-sec for the three-reaction wheel case. Hence all input to the control system must be smoothed by the command generator to prevent loop saturation and the resulting vehicle instability from initiating backup mode entry. During star-to-star maneuvers, the rate gyro assemblies are switched to their high rate range. To prevent excitation of the structural modes caused by increased rate gyro assembly pulse quantization, the pointing control system loop gain is dropped and the integral gain is set to zero. This action effectively drops the pointing control system bandwidth up to an order of magnitude, allowing adequate control during the maneuver, and limits structural excitation caused by rate gyro assembly quantization.

Disturbance torques, e.g., gravity gradient and aerodynamics, act upon the Space Telescope causing the wheel speeds of the reaction wheel assemblies to increase. To prevent the reaction wheels from reaching a saturated condition that would cause a loss of vehicle control, a momentum control system that manages the speed buildup in the reaction

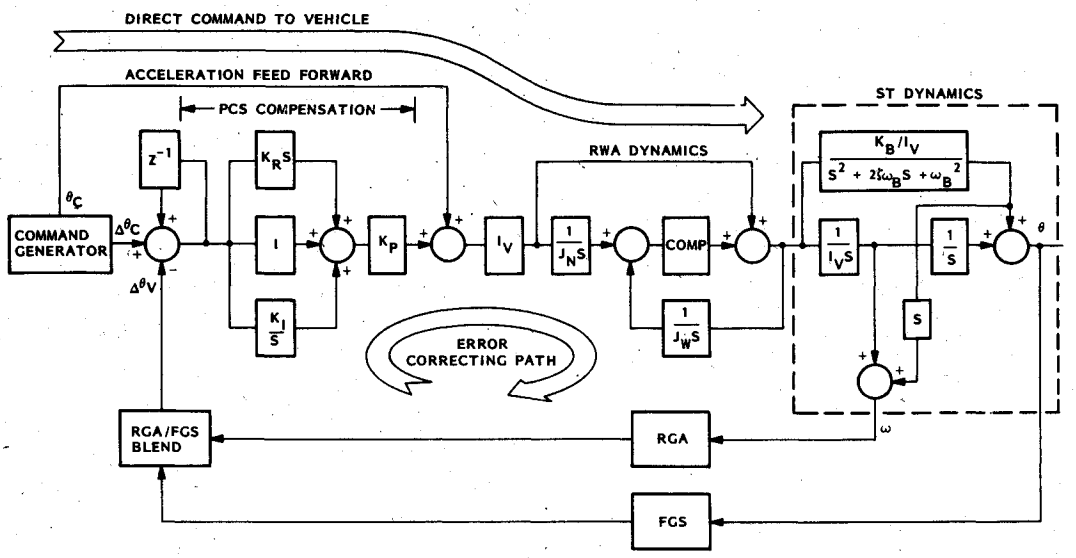


**Fig. 4 Simplified pointing control system.**

wheels is provided. Momentum control operates concurrently with the primary loop. This system uses the rate gyro assemblies for rate information, and uses a magnetometer or an onboard computer model of the Earth's magnetic field, and magnetic torquers for control torques. The primary momentum control law, called the minimum energy law, is based upon minimization of the energy dissipated in the torquer. The minimum energy law also provides minimal reaction wheel assembly speeds following vehicle maneuvers. In addition, the cross-product momentum management law is implemented, and is used following Shuttle Orbiter deployment and retrieval operation and in backup control operation. Both the minimum energy and cross-product law provide near-equal performance for long-term inertially fixed operation. The minimum energy law centers the peak reaction wheel speeds about zero. The minimum energy law provides better control of peak reaction wheel speeds following a maneuver, particularly in the three-reaction wheel situation, and provides a more rapid return to the steady-state wheel speeds following a maneuver.

### Stability Considerations Based on Structural Modes

The pointing control system compensation and sampling rate is selected to stabilize the system considering the solar array and optical telescope assembly bending modes. The criteria used to determine the suitability of the compensation and sample rate are the stability margins and system response time. The integral path in the control path causes the open-loop transfer function to be type 3; hence the loop is a conditionally stable design, i.e., instability results if the open-loop gain is increased or decreased too much. This fact gives rise to a low-frequency and high-frequency gain margin. The mode suppression refers to the gain attenuation achieved for high-frequency bending modes. The stability margin criteria used in the design are.

| | |
|---|---|
| Low-frequency gain margin: | ≥10 dB |
| High-frequency gain margin: | ≥ 6 dB |
| Phase margin: | ≥30 deg |
| Mode suppression (high frequencies): | ≥10 dB |

The pointing control system response time requirements lead to the specification of a 1-2 Hz bandwidth. There was some design flexibility available in specifying bending mode frequency bands. The solar array dominant frequencies are designed to be in the 0.05-0.7 Hz range. The lower limit is constrained by the required maneuver time (90 deg in 18 min or less), reaction wheel torquer size, and allowable structural mode excitation during a maneuver. The upper frequency

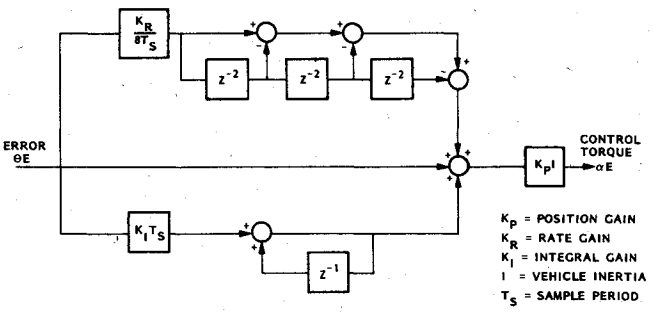


**Fig. 5 Pointing control system control law.**

limit is established by the pointing control system bandwidth and required stability margins. The optical telescope assembly structural frequencies are designed to be above 18 Hz to allow adequate stability margins and system response. The specification of the structural frequency is one of the few design parameters that can be controlled, as the parameters affecting the amplitude of the model gain, $K_B$, are essentially a fallout of the Space Telescope mass distribution and inertia properties. The model used for a bending mode is of the form:

$$\frac{\theta_B}{T_i} = \frac{K_B/I_j}{S^2 + 2\zeta_B\omega_B S_+ \omega_B^2}$$

where $\theta_B$ is bending angle output, $T_i$ is input torque, $K_B$ is bending mode gain, $I_j$ is vehicle inertia for the $j$th axis, $\zeta_B$ is damping (0.005), and $\omega_B$ is bending mode natural frequency (rad/s).

For a simple two-body system coupled by a spring of frequency $\omega_B$, the gain $K_B$ is the ratio of the inertia of the outer body to the controlled centerbody. For the Space Telescope, this analogy can be visualized where the solar array is the outer body and the system support module and optical telescope assembly are the centerbody. For the solar array, $K_B$ is less than or equal to 0.5, which indicates the solar array inertia could be one-half that of the centerbody. This is a large modal gain and has resulted in the Space Telescope design being tailored for stabilizing and limiting the structural excitation of the solar array.

The optical telescope assembly modes have $K_B$ values ranging from $-1$ for the system support module/optical telescope assembly fundamental scissor mode to values of up to $\pm 4$ for the higher frequency secondary mirror/primary mirror modes.

The Space Telescope control law proportional-integral-derivative compensation is shown in Fig. 5. The gains are

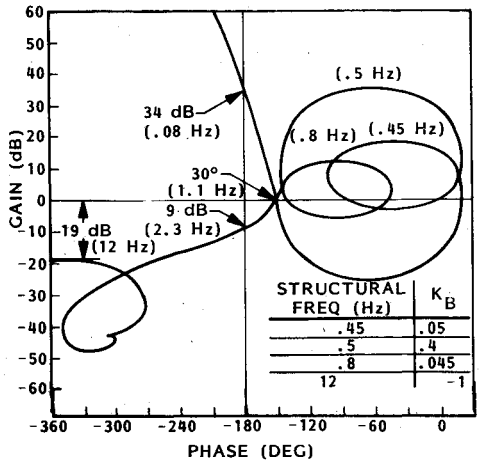


**Fig. 6 Linear stability analysis.**

chosen to meet bandwidth and stability margin requirements. To achieve the desired suppression of the coupled system support module/optical telescope assembly modes, the digital rate filter is used. The Nichol's chart for the resulting control law and filter network is shown in Fig. 6. As can be seen, all design criteria can be satisfied.

The overall sensitivity of the control law design to bending mode amplitude, i.e., $K_B$, was determined. A single bending mode is included in the pointing control system model. The bending frequency was fixed at various frequencies, and the value of $K_B$ was increased until the closed-loop roots in the $z$ plane crossed the unit circle. The limiting value of $K_B$ as a function of frequency is shown in Fig. 7. As shown, the stability characteristics are sensitive to the location of the Space Telescope bending modes. These sensitivity studies have been used in specifying the computer sample rate and the modal frequency ranges for the vehicle, particularly with regard to the solar array and optical telescope assembly, as discussed above. The computational rate of 40 Hz may seem high when the loop bandwidth is on the order of 1 to 2 Hz. However, detailed sensitivity studies show that lower rates degrade the phase margins at the lower frequencies and cause a dip in the modal sensitivity curve (shown in Fig. 7) around the low-frequency gain margin frequency, nominally 0.08 Hz. The sample rate is to maintain stability margins with the low-frequency bending modes. The dip in the stability bound above 20 Hz is due to a combination of frequency foldover (sampling frequency is 40 Hz) and the placement of the zeros of the rate filter, since frequencies above the half-sample frequency are folded about this frequency. As an example, a bending mode at 22 Hz appears at 18 Hz after being sampled at a 40-Hz rate. Thus, as the modal frequency increases above 20 Hz, it appears at a lower frequency in the sampled spectrum. Above approximately 25 Hz, attenuation of the sampled signal results from the fact that as the frequency of the input signal approaches the sampling frequency, there are not enough samples during each period to accurately reconstruct the input.

Various forms of compensation filters were considered. Analog filters are not appropriate as the speed of response of the system depends on a direct acceleration command path to the reaction wheels; hence a filter cannot be placed on the hardware. Also, it was deemed advisable to maintain the compensation in the computer to allow computer data base change of filter values as the vehicle bending modes are defined in system test. The compensation is constrained since: 1) the forward loop gain, $K_p$, must be high to counter reaction wheel bearing friction and provide adequate stability for low-frequency solar array modes; 2) the integral compensation path is needed to attenuate low-frequency disturbance torques such as gravity gradient and aerodynamic; 3) the bandwidth is approximately 1-2 Hz; and 4) the high-frequency structural

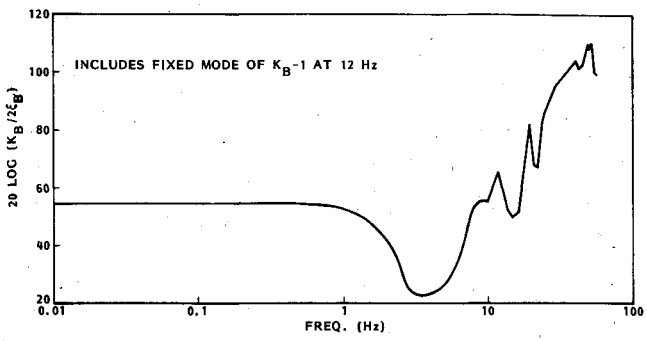


**Fig. 7 Modal sensitivity.**

modes, e.g. the scissor mode, must be attenuated at least 10 dB. Butterworth filters contributed too much phase lag; notch filters proved ineffective. The digital rate filter shown in Fig. 5 demonstrated the proper stability characteristics and the flexibility to be adjusted for scissor mode frequency.

In summary, the analysis of the primary pointing control system loop indicates design performance can be achieved. In addition, possible modifications required as structural data matures can be handled by change of control parameters without a major redesign of the control law.

## Minimum Energy Momentum Management

The momentum management system incorporates a minimum energy desaturation law that bounds the reaction wheel speed, thereby maximizing residual wheel momentum available to accomplish maneuvers. While the minimum energy law results in the smallest amount of energy required for the desaturation process, the minimum energy formulation's primary utility is in yielding a control law that allows an effective algorithm for limiting reaction wheel speeds and ensuring rapid return of the speed to steady-state levels following star-to-star maneuvers.

The minimum energy law minimizes the energy dissipated in the magnetic torquers over a specified time interval, subject to the constraint that the momentum vector generated by the sum of the gravity gradient and magnetic torques is equal to the change in the reaction wheel momentum vector. Ideally, the sum of the gravity and magnetic torque components is zero, and no reaction wheel momentum buildup occurs. This ideal condition is not achieved over short intervals, as the magnetic torque is the cross product of the Earth's magnetic field and the torquer magnetic moment. Hence the reaction wheel speeds will not be zero. The minimum energy law uses energy proportional to the amount of the bias momentum to be dumped during a desaturation interval, and does not attempt to reduce the nominal cyclic momentum. In the ideal case, the energy used will be proportional to the bias gravity gradient torque magnitude. Because of the nominally cylindrical distribution of Space Telescope inertia, the energy used is proportional to the angle that the optical axis, $V_I$, makes with respect to the orbit plane, peaking when the optical axis is 45 deg to the orbital radius vector. When the optical axis is in the orbit plane, there is negligible bias torque and, therefore, essentially zero energy dissipated in the torquers.

The minimum energy law generates commands based on the specified desaturation interval; hence it is an open-loop control law by nature; i.e., it does not accept feedback information within the desaturation interval. The minimum energy law is subject to sensitivity effects, such as undetected magnetic coil failures and estimation errors in the models of the geomagnetic field and the gravity gradient torques. These sensitivities can be greatly reduced by using a desaturation interval of 900 s with 300-s updates (i.e., every 300 s, the magnetic commands are recomputed based on a new 900-s desaturation interval). Essentially, the updates close the loop every 300 s. The 900-s desaturation interval with 300-s up-

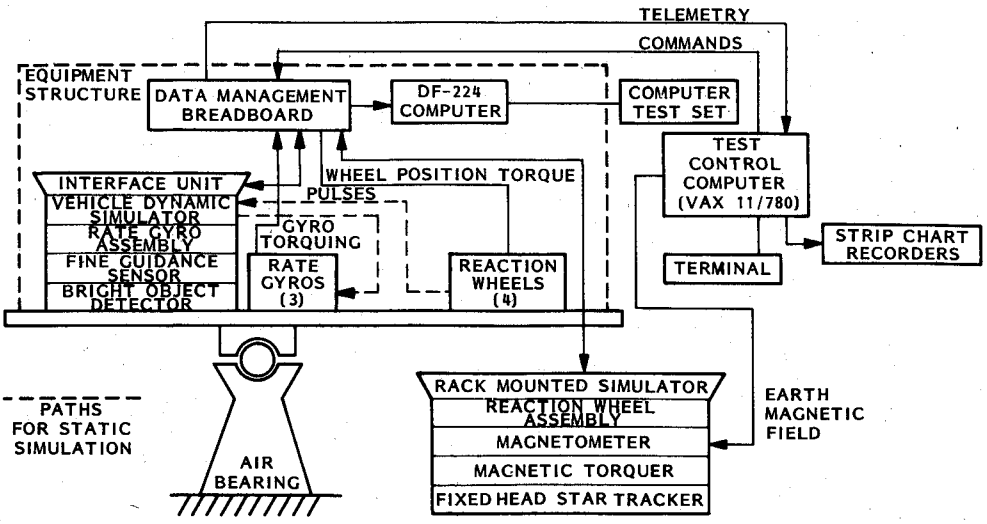


**Fig. 8 Space Telescope development test setup.**

dates are used in the minimum energy law during star observations.

During star-to-star maneuvers, in place of the 900- and 300-s intervals, a single long interval equal to the maneuver time plus lead and lag times is used. The lead and lag times are introduced to allow more time for magnetic field variation in order to dump the required momentum. Typically, the lead and lag times are 500-1000 s. This is particularly important when the geomagnetic field has small variation in direction along the Space Telescope orbit path or is of low magnitude such as in the region of the South Atlantic Anomaly. A measure of difficulty during any desaturation time interval is the angle between the magnetic field vector and the momentum to be dumped. When these vectors are nearly parallel, the torquer magnetic moment commands become high, since no magnetic torque can be produced in the direction of the magnetic field vector. The longer desaturation interval introduced by the lead and lag times prevents the torquers from extended periods of saturation. Even though the torquers are not desaturating the instantaneous momentum buildup during the lead and lag times, the system is ensuring that the reaction wheel speeds following the maneuver are minimal and reach steady state within a short settling time.

The minimum energy law calculates the torquer magnetic moment needed to counteract the effect of the bias gravity gradient torques only. The law ensures centering of the cyclic components by generating a nominal momentum profile for each interval. The minimum energy control law is derived by minimizing the energy lost in the coils using calculus of variations to minimize that performance parameter.

Before the start of each desaturation interval, the costate vector is computed on the basis of 1) the geomagnetic field, 2) the reaction wheel momentum at the beginning and the desired value at the end of the desaturation interval, 3) the vehicle momentum, and 4) the gravity gradient torque. The value of the costate vector then is used to compute the magnetic dipole moment for each coil throughout the desaturation interval. Nominally, the difference between the desired momentum at the beginning and end of the interval and the integral of the gravity gradient torque is effectively the momentum caused by the gravity gradient bias torque.

## Development Testing

Pointing control system development testing at the subsystem level is structured as a two-phase test approach consisting of pointing control system testing performed initially under static conditions, followed by dynamic tests. The overall test philosophy is one of progressive testing of the hardware-software interface between the data management system and the complement of pointing control system sensors and actuators. The concept of testing via simulated hardware is used extensively during the static phase. A pointing control system functional simulator has been developed specifically to support testing.

The test objectives are to demonstrate 1) hardware-software interface compatibility, 2) the validity of the hardware-software models used in the pointing control system analysis and simulation, and 3) the functional simulation test cases to be used in Space Telescope system testing. Certain static test cases used in development testing will be carried forth to Space Telescope flight system testing to allow continuity of test results between development and flight testing.

The pointing control system functional simulator has the following characteristics.

1) *Hardware simulators:* Pointing control system component mathematical models implemented in discrete electronic component form; each hardware simulator is modularized and replicates the hardware interface with the data management system, permitting substitution of any combination of simulators for their respective flight-type hardware counterparts during test. For example, the engineering models of the reaction wheel and rate gyros can be substituted for a model in the simulator during the static tests. Essentially, every pointing control system hardware element has been simulated in the functional simulator.

2) *Vehicle dynamics simulation:* The vehicle dynamics simulator module provides an electronic simulation of vehicle motion for closed-loop testing under static conditions. The input is reaction wheel incremental angle pulses. The vehicle dynamics simulator converts this to an equivalent vehicle rate command to the simulated torquing input to the rate gyro hardware.

The static test phase demonstrates the primary pointing control system functional requirements: momentum management, maneuvering, pointing, control, and stabilization and attitude update. Hardware-software interface compatibility also is demonstrated. The engineering model reaction wheel and engineering model/flight spare rate gyro can be substituted into the simulation to demonstrate compatibility with the hardware. At the conclusion of the static phase hardware-software compatibility, momentum management, attitude update, and preliminary fine pointing model verification will be demonstrated. Fine pointing operations, e.g., maneuvers, fine guidance sensor acquisition, star observation, solar object tracking, and scanning, together with model verification, will be demonstrated to the level compatible with the functional simulation capability. In general, fine pointing test cases run during the static phase will be carried forward to Space Telescope system testing.

The dynamic testing is directed toward fine pointing modes such as star observation and solar object tracking. The testing

is performed on a three-axis airbearing table, Fig. 8. The test uses one engineering model, two flight reaction wheels, the engineering model/flight spare, one flight rate gyro, and the functional simulator to emulate the fine guidance sensor. The test cases will be run to evaluate hardware and software models. The digital and hybrid computer results, functional simulator results, and airbearing results will be compared, discrepancies will be resolved, and models will be updated where required.

The resolution available for verifying models using the functional simulator is in the range of 0.005 to 1 arc-sec, depending on the scaling used for gyro and reaction wheel quantization. The airbearing results are expected to be 0.03 arc-sec or better.

## Conclusions

Certain key features of the Space Telescope's pointing control system have been addressed. An overview of the pointing control system operations scenario, hardware and software complement, momentum mangement, and development test program was given. Design drivers such as structural modes and dynamic control range were discussed. The selection of control system sample rate and compensation, and the inherent flexibility provided to adapt to structural modes were discussed.

## Acknowledgments

This work was sponsored by the NASA Marshall Space Flight Center, Huntsville, Ala., under Contract NAS8-32697.

## References

[1]Field, E.L., "Space Telescope, A Long-Life Free Flyer," Paper 79-228 presented at the Annual Meeting of the American Astronautical Society, Los Angles, Calif., Oct. 29-Nov. 1, 1979.

[2]Bahcall, J.N. and O'Dell, C.R., "The Space Telescope Observatory," NASA TM-78301, June 1979.

[3]Wissinger, A., "Design Constraints of the LST Fine Guidance Sensor," Paper 75-1072 presented at the AIAA Guidance and Control Conference, Boston, Mass.

[4]Glaese, J.R., Kennel, H.F. Nurre, G.S., Seltzer S.M., and Shelton, H.L., "Low-Cost Space Telescope Pointing Control System," *Journal of Spacecraft and Rockets*, Vol. 13, July 1976, pp. 400-405.